



ELSEVIER

Journal of Physics and Chemistry of Solids 61 (2000) 1901–1911

JOURNAL OF  
PHYSICS AND CHEMISTRY  
OF SOLIDS

www.elsevier.nl/locate/jpcs

# Stability, electronic structure and reactivity of the polymerized fullerite forms

V.V. Belavin<sup>a</sup>, L.G. Bulusheva<sup>b,\*</sup>, A.V. Okotrub<sup>b</sup>, D. Tomanek<sup>c</sup><sup>a</sup>Novosibirsk State Technical University, av. Karla Marksa 20, Novosibirsk 630092, Russia<sup>b</sup>Institute of Inorganic Chemistry SB RAS, av. Ak.Lavrenteva 3, Novosibirsk 630090, Russia<sup>c</sup>Department of Physics and Astronomy, Michigan State University, East Lansing, MI 48824-1116, USA

Received 1 January 2000; accepted 3 April 2000

## Abstract

A study of band structure, stability and electron density distribution from selected crystal orbitals of polymerized C<sub>60</sub> forms was carried out. Linear chain, tetragonal and hexagonal layers, and three-dimensional (3D) polymer with a simple cubic lattice were calculated using an empirical tight-binding method. The hopping parameters were chosen to fit a theoretical X-ray emission spectrum of C<sub>60</sub> to the experimental one. Our results indicate that all calculated polymers are semiconductors with the smallest energy gap for hexagonal structure. Though the molecules C<sub>60</sub> are linked by strong covalent bonds, the crystal orbitals characterized by the electron density localization on an individual carbon cage are separated in the electronic structure of polymers. The suggestions about reactivity of the 1D and 2D tetragonal polymers were made from the analyses of crystal orbitals accompanied with the highest occupied (HO) and lowest unoccupied (LU) bands. The polymerized C<sub>60</sub> forms were found to be less stable than an icosahedral fullerene molecule. © 2000 Elsevier Science Ltd. All rights reserved.

**Keywords:** A. Polymers; D. Electronic structure

## 1. Introduction

At ambient conditions solid C<sub>60</sub> is a molecular crystal, in which the molecules are orientationally disordered while their centers of mass form a regular face-centered-cubic (fcc) lattice. At higher temperature and pressure, the fullerite C<sub>60</sub> is polymerized forming the various crystal structures depending upon the synthetic conditions [1–5]. Treatment of the fullerite in the pressure range below 8 GPa and at temperature about 750 K results in the formation of linear C<sub>60</sub> chains along the (110) direction of the original fcc lattice leading to an orthorhombic phase. Increasing the temperature provides an additional intermolecular bonding in either (111) or (100) planes, and the synthesis of a rhombohedral or tetragonal phase. These phases have a two-dimensional (2D) structure with the interlayer distance of 9.8 Å [2,3]. Above about 8 GPa very hard, 3D polymeric structures are formed [6].

Studies by IR-, NMR and Raman spectroscopy showed the lowering in symmetry of the fullerene molecules and the

presence of sp<sup>3</sup> intermolecular bonds in the polymerized C<sub>60</sub> structures. The molecules C<sub>60</sub> are linked with each other by [2 + 2] cycloaddition mechanism forming a four-membered ring between the neighbors [7–9]. Strong covalent bonding between the cages and, as a consequence, the reduction of number of π-electrons in C<sub>60</sub> change the electronic properties of the fullerite. Thus, the bands in the photoemission spectrum of polymerized C<sub>60</sub> film are shifted toward the Fermi level [10] decreasing the energy gap relative to that of the fullerite. At present, the techniques of producing the polymeric phase in the pure form and the quantities, sufficient for an experimental research of their electronic properties, are still developing. In this connection, a study of the electronic structure of polymers by quantum chemistry is very important for prediction of their possible properties and applications.

From tight-binding calculation, a linear C<sub>60</sub> chain has been found to be semiconductive with a finite band gap of 1.148 eV and almost pure σ-type intermolecular bonding [11]. Assuming the weak van der Waals interlayer interaction in the rhombohedral and tetragonal polymers, a theoretical prediction on stability and conducting properties of

\* Corresponding author.

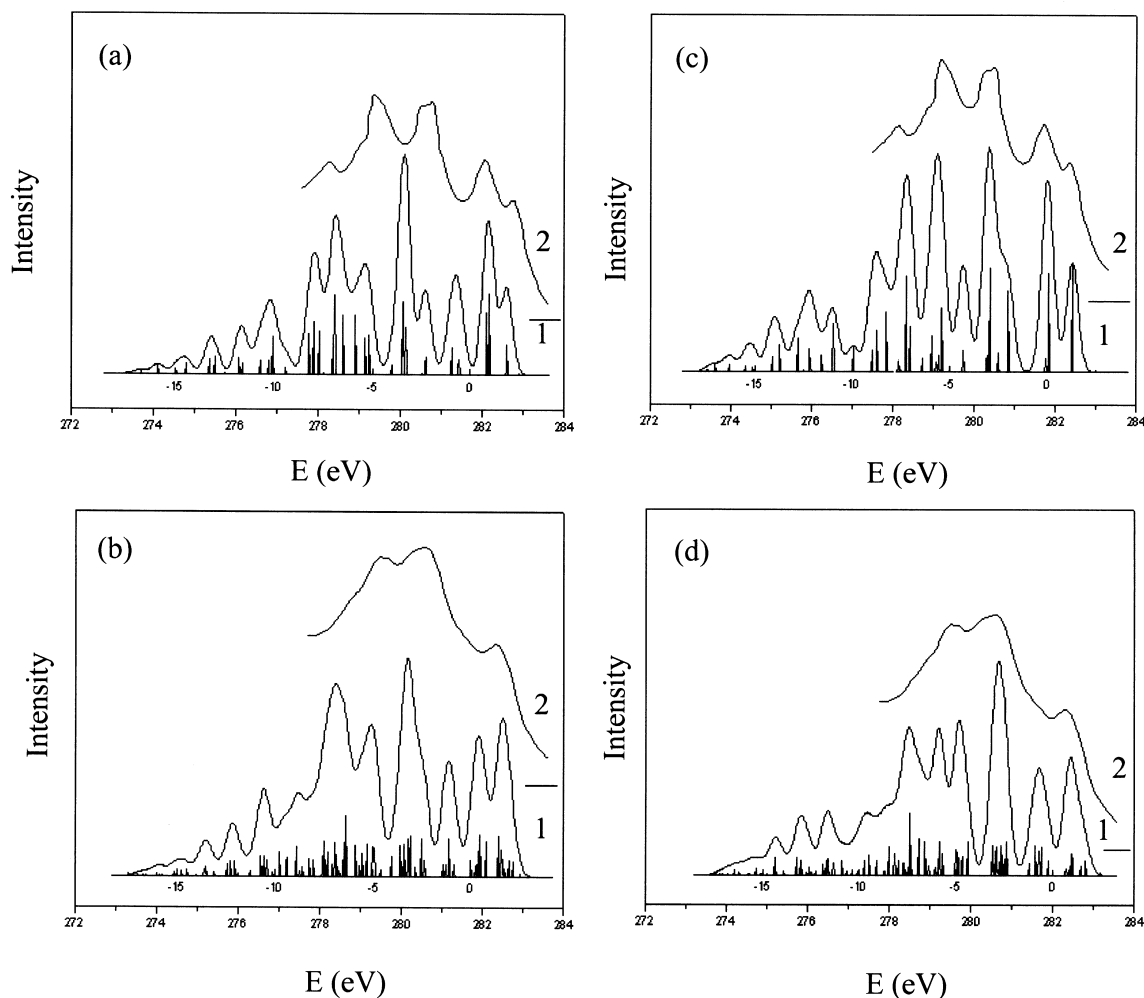


Fig. 1. Comparison of the theoretical  $CK\alpha$  spectra (profile 1) of  $C_{60}$  and  $C_{70}$  calculated with the old (a,b) and new (c,d) parametric set with the experimental X-ray spectra (profile 2) of the fullerite  $C_{60}$  (a,c) and  $C_{70}$  (b,d).

these phases have been made by the result of tight-binding calculation of a single layer [12]. Different number of intermolecular covalent bonds in the tetragonal and rhombohedral structures was found to cause the distinction of band gap values, which were estimated to be 1.2 and 1.0 eV, respectively. The investigation of the electronic structure of the 3D rhombohedral and tetragonal  $C_{60}$  polymers has been carried out in Refs. [13,14] using the local-density approximation (LDA). These phases were found to be elemental semiconductors having indirect gaps of 0.35 and 0.72 eV. Although the LDA generally underestimates the energy gap, its value is consecutively reduced from the  $C_{60}$  to the rhombohedral phase, that correlates well with the result of tight-binding calculations [12]. Furthermore, as theoretically predicted it is possible to synthesize a three-dimensionally polymerized metallic fullerite under pressure of about 20 GPa [15].

The goal of present contribution is to study the electronic

band structure, stability and chemical bonding of the  $C_{60}$  solids with the framework of a uniform quantum-chemical approach. All polymers known to date: 1D, 2D tetragonal, 2D hexagonal and 3D cubic structures are considered. The polymers are calculated using an empirical tight-binding method, which was specially parameterized to reproduce correctly the electronic density of states (DOS) in the valence band of fullerenes  $C_{60}$  and  $C_{70}$ .

## 2. Computational details

Using an empirical tight-binding approach to study an electronic structure of any compound, it is necessary to choose matrix elements for correct description of the interelectronic interactions. As the fullerite is an allotropic form of carbon, the parameters obtained by fitting the band structure of bulk graphite were used as the initial ones [16].

Table 1  
Parameters for the functions  $s(r)$ ,  $\phi(r)$  and coefficients of the polynomial  $f(x)$

$n$	$n_c$	$r_c$ (Å)	$r_0$ (Å)		
2.0	6.5	2.18	1.536		
$\phi_0$ (eV)	$m$	$m_c$	$d_c$ (Å)	$d_0$ (Å)	
4.165	4.203	8.185	2.105	1.640	
$c_0$	$c_1$	$c_2$	$c_3$	$c_4$	
-2.590	0.572	$-1.789 \times 10^{-3}$	$2.353 \times 10^{-5}$	$-1.242 \times 10^{-7}$	

These parameters were checked against the X-ray fluorescence spectra of fullerites  $C_{60}$  and  $C_{70}$  [17].

An X-ray emission arises as a result of electron transitions from valence shell of a compound to core-located vacancies. As these transitions are governed by the dipole selection rules, CK $\alpha$  spectrum corresponds essentially to the density of states of carbon 2p electrons. The theoretical CK $\alpha$  spectra of  $C_{60}$  and  $C_{70}$  were plotted by the results of tight-binding calculations of the fullerenes molecules. A comparison between the experimental spectrum of fullerite and the theoretical spectrum of free molecule is possible because of the weakness of intermolecular interactions in the solids, as evident from the insignificant band dispersion in the fullerite  $C_{60}$  [18]. The intensity of a separate spectral line was calculated as a sum of squared modules of the coefficients with which 2p-atomic orbitals (AO) contribute in the molecular orbital (MO). For each occupied MO, the calculated contribution is represented as a line, which position on the energy scale within the Koopmans' theorem gives the one-electron energy of corresponding MO. The resulting spectral profile was obtained by broadening the vertical lines by a 0.3-eV full-width-at-half-maximum Gaussian function.

Comparison between the experimental CK $\alpha$  spectra of fullerites  $C_{60}$  and  $C_{70}$  and the theoretical spectra of molecules calculated with the parameters set [16] is shown in Fig. 1(a and b). The theoretical spectra profiles do not correlate with the experimental ones in the one-electron energy region below 0. The reasons of such discrepancy were found from the analysis of calculation results to be inadequate interaction of the  $\pi$ -electrons and the underestimating of s- and p-states hybridization of in the cage fullerene molecules. The hopping parameters  $V_{pp\pi}$  and  $V_{sp\sigma}$ , which are responsible for these interactions, were fitted to the best agreement between the theoretical and experimental X-ray spectra of  $C_{60}$ . The spectrum of  $C_{60}$  molecule, calculated with a set of parameters  $E_s = -3.65$  eV,  $E_p = -3.65$  eV,  $V_{ss\sigma} = -3.63$  eV,  $V_{sp\sigma} = -4.50$  eV,  $V_{pp\sigma} = -5.38$  eV,  $V_{pp\pi} = -3.04$  eV, reasonably reproduces the number of main spectral features, their relative intensities and energy separations in the experimental spectrum (Fig. 1(c)). Using the new parameter set, we calculated the CK $\alpha$  spectrum of  $C_{70}$  molecule. Quite well agreement between experimental and theoretical spectra for this compound (Fig. 1(d)) confirms the ability of chosen parameters to correctly describe the electron interactions in fullerenes molecules. These parameters would be expected to take into account

the specificity of cage carbon structures such as spatial peculiarities and electronic states of atoms.

The total energy of the carbon systems was calculated as:

$$E_{\text{tot}} = E_{\text{bs}} + E_{\text{rep}}, \quad (1)$$

where  $E_{\text{bs}}$  is the sum of electronic eigenvalues over all occupied electronic states and  $E_{\text{rep}}$  is a short-ranged repulsive energy. The electronic eigenvalues are obtained by solving the empirical tight-binding Hamiltonian, the off-diagonal elements of that  $V_{ss\sigma}$ ,  $V_{sp\sigma}$ ,  $V_{pp\sigma}$ , and  $V_{pp\pi}$  were scaled with interatomic separation  $r$  as a function  $s(r)$ . The repulsive energy  $E_{\text{rep}}$  was calculated using the expressions given in Ref. [19]:

$$E_{\text{rep}} = \sum_i f \left( \sum_j \phi(r_{ij}) \right), \quad (2)$$

where  $\phi(r_{ij})$  is pairwise potential between atoms  $i$  and  $j$ , and  $f$  is a functional expressed as a fourth-order polynomial. The pairwise potential  $\phi(r)$  and scaling function  $s(r)$  are parametrically expressed by [20]:

$$\phi(r) = \phi_0 \cdot (d_0/r)^m \cdot \exp(m \cdot (-r/d_c)^{m_c} + (d_0/d_c)^{m_c}) \quad (3)$$

$$s(r) = (r_0/r)^n \cdot \exp(n \cdot (-r/r_c)^{n_c} + (r_0/r_c)^{n_c}) \quad (4)$$

The change of  $V_{sp\sigma}$  and  $V_{pp\pi}$  values required of the re-parameterization of these functions. The parameters were chosen by fitting the dependence of cohesive energy versus nearest-neighbor interatomic separation for graphite and diamond [20]. The resulting parameters for the functions  $\phi(r)$  and  $s(r)$  and the polynomial coefficients are given in Table 1. Using these parameters gave the bond lengths of 1.542 and 1.446 Å in diamond and graphite at equilibrium. These values satisfactorily correlate with the experimental ones 1.546 and 1.420 Å, respectively.

Electronic DOS was calculated by a histogram method, in which an energy interval is split into the cells with width of  $\Delta E$ , and number of states  $N_i$  is computed in each of the cells. The integration over the irreducible wedge of the Brillouin zone was done using 36  $k$  points and 0.1-eV Gaussian broadening.

### 3. Results and discussion

1D, 2D tetragonal and hexagonal polymers of  $C_{60}$  are depicted in Fig. 2. The neighboring fullerene cages are

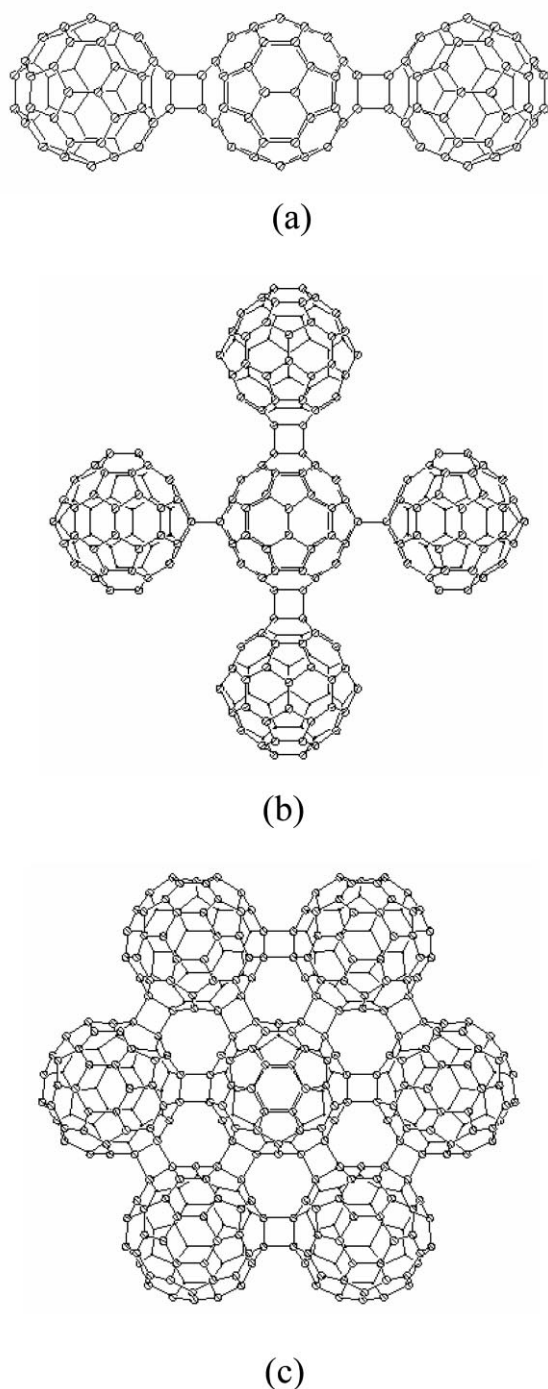


Fig. 2. The fragments of linear  $C_{60}$  chain (a), 2D tetragonal (b) and hexagonal (c) polymers.

linked by the four-membered rings from carbon atoms at a fusion between two hexagons of a molecule. Each  $C_{60}$  molecule in the polymeric chain is connected to two neighbors and belongs to symmetry point group  $D_{2h}$ . In the tetragonal

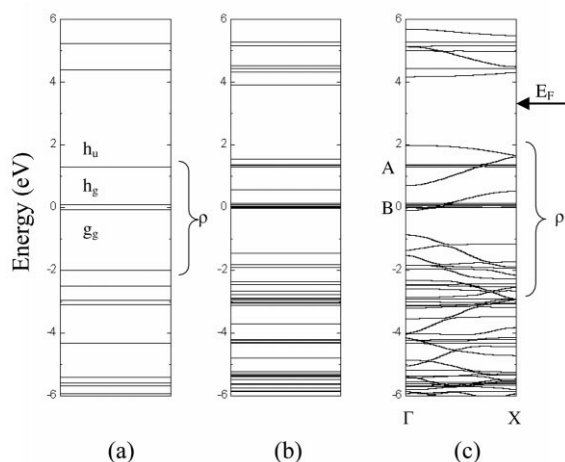


Fig. 3. Energy levels of the icosahedral  $C_{60}$  molecule (a), the distorted  $C_{60}$  cage from the linear polymer (b), and the band structure of the linear  $C_{60}$  polymer (c). The small-dispersed occupied bands are marked by A and B.

and hexagonal layers, each individual molecule having four or six neighbors belongs to the symmetry point group  $D_{2h}$  or  $D_{3d}$ , respectively. 3D cubic polymer was constructed by the attachment of two  $C_{60}$  molecules in perpendicular direction to the tetragonal layer. The atomic coordinates in the distorted carbon cages were obtained from the results of geometry optimization of a linear trimer  $(C_{60})_3$  by quantum-chemical semiempirical PM3 method [21]. A unit cell of the polymeric chain is the central  $C_{60}$  fragment of the trimer. The geometry of this fragment has the most deviation from an icosahedral one near the four-membered rings. Conserving this deviation near each linking ring, the atomic coordinates for other polymers were generated according to the point group symmetry of  $C_{60}$  cage in a unit cell. An intramolecular bond length of 1.55 Å taken also from Ref. [21] is characteristic for the carbon compounds in the  $sp^3$ -hybridization.

### 3.1. Linear $C_{60}$ chain

Molecular orbitals of the icosahedral  $C_{60}$  may be divided into two types: radial  $\rho$ -orbitals directed towards the center of the carbon cage and tangential  $\tau$ -orbitals aligned with the local normal of the cage surface. According to the results of calculation using various quantum-chemical methods, the highest occupied MO (HOMO) of fullerene is a fivefold degenerated orbital with  $h_u$  symmetry and the lowest unoccupied MO (LUMO) is a threefold orbital with  $t_{1u}$  symmetry. These MOs are  $\rho$ -type orbitals. Distortion of the fullerene molecule during polymerization changes its electronic structure. The energy levels of icosahedral  $C_{60}$  and the  $C_{60}$  fragment isolated from the linear chain are compared in Fig. 3. A deviation from the icosahedral structure causes the splitting of the degenerated MOs and, therefore, the energetic

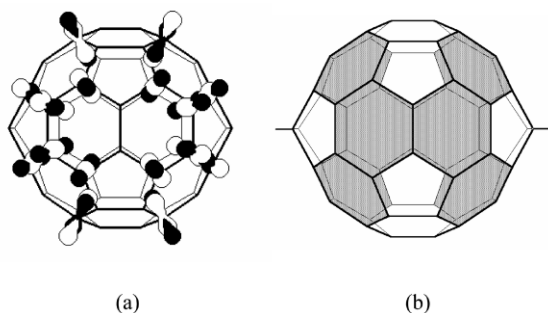


Fig. 4. Schematic structure of the crystal orbital (a) corresponding to the small-dispersed band of the linear C<sub>60</sub> chain, the electron density from such type orbital is mainly localized on dashed hexagons (b).

broadening of  $\rho$ - and  $\tau$ -orbital blocks. The splitting depends on the extent of molecular distortion.

The covalent bonding of the C<sub>60</sub> cages in the polymeric chain results in the dispersion of energy levels (Fig. 3(c)). The characteristic peculiarity of the polymer valence band is the presence of two groups, A and B, of crystal orbitals (CO) accompanied with the bands having very little dispersion. The pattern of electron density distribution for one of such COs is depicted in Fig. 4. Electronic density from this  $\rho$ -type orbital is mainly localized on twelve hexagons of carbon cage, while on the atoms providing the intermolecular bonding it is practically equal to zero. The number of similar localized COs may be suggested to depend on the extent of C<sub>60</sub> cage distortion and the crystal structure of a polymer.

According to the band structure calculation, the linear C<sub>60</sub> chain is a semiconductor. A direct band gap at the  $\Gamma$  point is about 2.180 eV; therefore, the polymer chain formation narrows the icosahedral C<sub>60</sub> HOMO–LUMO gap by 0.921 eV. The HO and LU bands of C<sub>60</sub> chain are not degenerate. Width of the LU band is about 0.125 eV indicating a small value of the transfer integral of  $\rho$ -electrons along the polymer chain. As the LU band is separated from higher states by 0.131 eV, the electron doping of the 1D C<sub>60</sub> polymer will make a single-band conducting system.

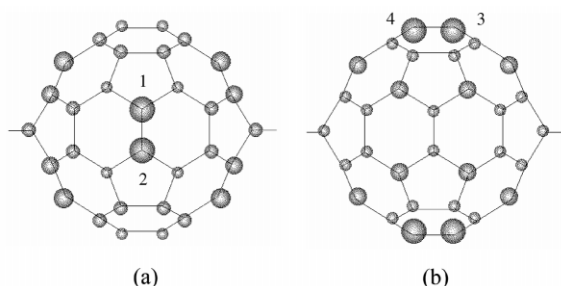


Fig. 5. Schematic representation of the frontier occupied (a) and unoccupied (b) orbitals of the linear C<sub>60</sub> chain. A circle size correlates with the 2p-AO participation in the construction of a given MO.

Analysis of the electron density distribution from the COs accompanied with the HO and LU bands (Fig. 5) can predict the reactivity of C<sub>60</sub> polymer. The atomic size is proportional to the sum of squared coefficients with which carbon AOs participate in the CO formation. The higher electron density on atoms 1, 2 for the HO and 3, 4 for the LU crystal orbitals will result in the further attachment of C<sub>60</sub> molecules to the double bonds with formation of the 2D tetragonal polymer.

### 3.2. 2D tetragonal polymer

The calculated band structure of the 2D tetragonal polymer near the Fermi level is shown along the symmetric direction of the square Brillouin zone (Fig. 6). The top of the valence band is found to be at the center of the Brillouin zone and the bottom of the conduction band is at the M point. The fundamental energy gap between these band extremes is 1.852 eV. The LU band in the tetragonal polymer is separated from higher states as that in the polymer chain, though its dispersion increases up to 0.286 eV indicating the stronger intramolecular overlapping of  $\rho$ -electrons. Two blocks of COs (A and B) characterized by the localization of electron density on the individual C<sub>60</sub> cages are positioned in the energy interval from 2 to 0 eV. Increasing the neighboring molecules in the tetragonal polymer reduces the total number of localized orbitals in the valence band near the Fermi level compared to the linear C<sub>60</sub> chain.

Structure of the frontier COs is schematically shown in Fig. 7 Both orbitals are characterized by the higher electron density on the central double bonds of a C<sub>60</sub> fragment. Therefore, we expect the attachment of the additional fullerene molecules to the tetragonal structure along  $z$  direction in the chosen coordinate system (Fig. 6) with the formation of 3D cubic polymer. Low electronic density on atoms 3 and 4 explains the small dispersion along the XM direction for the highest branch of the valence band.

### 3.3. Cubic polymer

The consideration of the 3D cubic polymer after the 2D tetragonal is caused by the increasing of a coordination number within the same point group symmetry of the C<sub>60</sub> fragment. In the cubic polymer, the C<sub>60</sub> cage being  $D_{2h}$  symmetric has the greatest number of neighbors. The band structure calculation shows that the cubic polymer has a direct energy gap of 2.235 eV at M point of the Brillouin zone (Fig. 8). Increasing the neighbors up to six in the polymer extends the energy gap by 0.05 and 0.38 eV in comparison with the 1D and 2D tetragonal structure, respectively.

The formation of covalent bonds along the additional direction enhances the intramolecular overlapping of  $p$ -electrons, and, therefore, their energy broadening. As the consequence the energy dispersion of the LU band increases up to 0.956 eV and, furthermore, all the unoccupied states form one continuous conduction band. Electronic structure

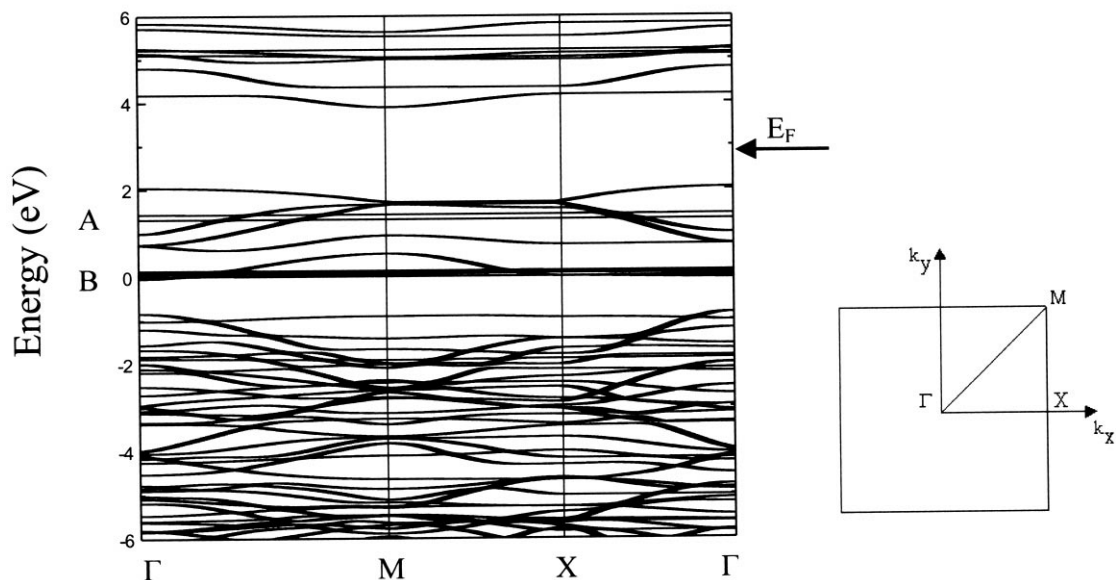


Fig. 6. Calculated band structure of the tetragonal polymer. The small-dispersed bands near the Fermi level are marked by A and B. The Brillouin zone corresponding to the  $C_{60}$  monolayer is also shown.

of the cubic polymer is characterized by the further narrowing of the energy interval in which the higher occupied bands are positioned. Among these bands only small-dispersed bands (A and B) are selected. The fifth and sixth neighbors in the cubic polymer are attached to the bonds shared by the central hexagons, that remains in the structure of the  $C_{60}$  fragment only eight slightly deformed hexagons. The  $\rho$ -electronic density is localized on these small sections (Fig. 9), while in the 1D and 2D tetragonal polymers the  $\rho$ -electrons are distributed on the areas composed of six adjacent hexagons. Spatial separation of the  $\rho$ -electrons in the cubic polymer reduces their intermolecular interaction that results in the narrowing of the higher occupied bands distribution.

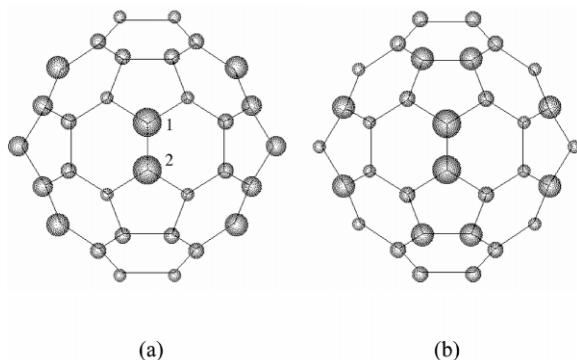


Fig. 7. Schematic representation of the frontier occupied (a) and unoccupied (b) orbitals of the tetragonal  $C_{60}$  polymer. A circle size correlates with the 2p-AO participation in the construction of a given MO.

### 3.4. 2D hexagonal polymer

Among the considered polymeric structures, the 2D hexagonal polymer is the most intriguing because of the high-symmetry  $C_{60}$  fragment is strongly distorted around the molecular equator due to the formation of 12 covalent bonds. The band structure of the hexagonal polymer is shown in Fig. 10. The polymer has indirect 0.577 eV gap between the extremes at K and T points. This value is minimal in the series of calculated  $C_{60}$  polymers. The LU and HO bands are twofold-degenerated in the center of the Brillouin zone. The bands of the polymer show considerable dispersion along all symmetry directions. Only one small-dispersed band near 0 eV can be selected. The electronic density from the CO corresponding to this band is localized on the areas composed of four adjacent hexagons from the top and bottom parts of the  $C_{60}$  fragment (Fig. 11). The  $\rho$ -electrons of the COs accompanied with the HO and LU bands were found to localize on the tops of the slightly deformed pentagons. The  $C_{60}$  fragments in the hexagonal layer are closely packed that makes it possible to the intermolecular interaction of  $\rho$ -electrons through the small tetragonal cavities. It is the reason of the large dispersion of the HO and LU bands along the  $\Gamma K$  direction of the Brillouin zone.

### 3.5. Analysis of electronic density of states

The calculated electronic DOS for the icosahedral  $C_{60}$  molecule and the polymerized  $C_{60}$  structures are compared in Fig. 12. The electron distribution near the Fermi level is the most interesting. The feature A in the DOS of  $C_{60}$  molecule

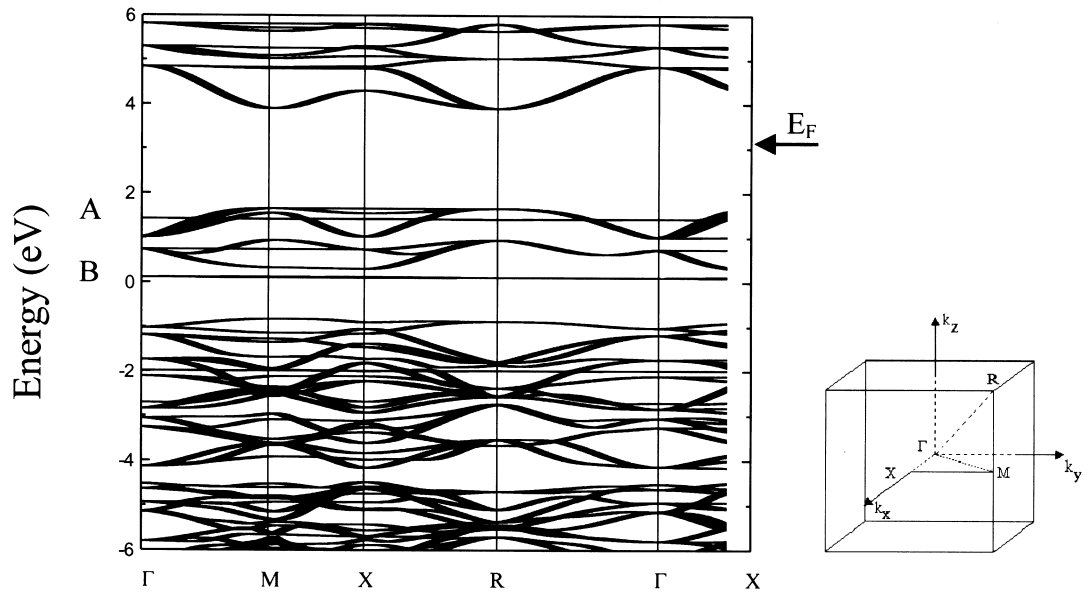


Fig. 8. Calculated band structure of the 3D  $C_{60}$  polymer. The first Brillouin zone of the simple cubic lattice is also shown.

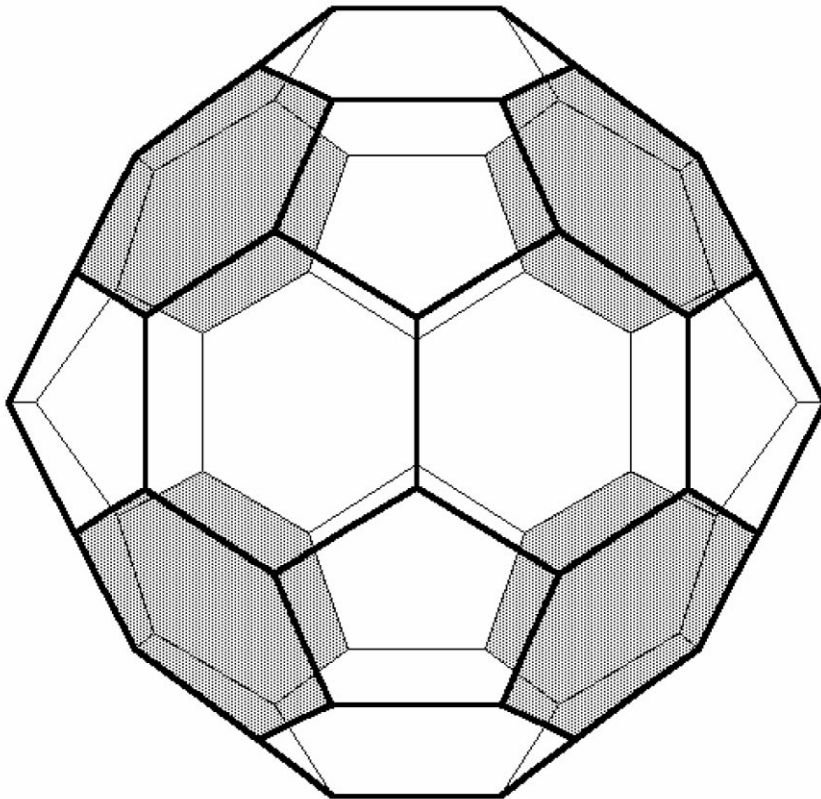


Fig. 9. Schematic representation of the crystal orbitals accompanied by the bands, which are marked by A and B in Fig. 8. The hexagons, on which the electron density is localized, are dashed.

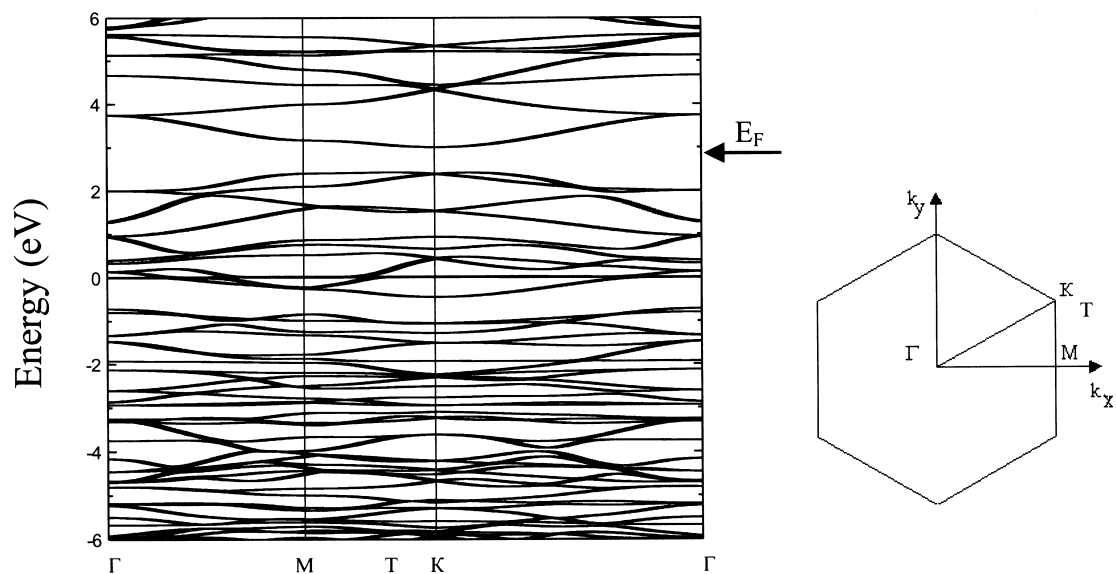


Fig. 10. Calculated band structure of the hexagonal  $C_{60}$  polymer around the Fermi level. The 2D Brillouin zone is also shown.

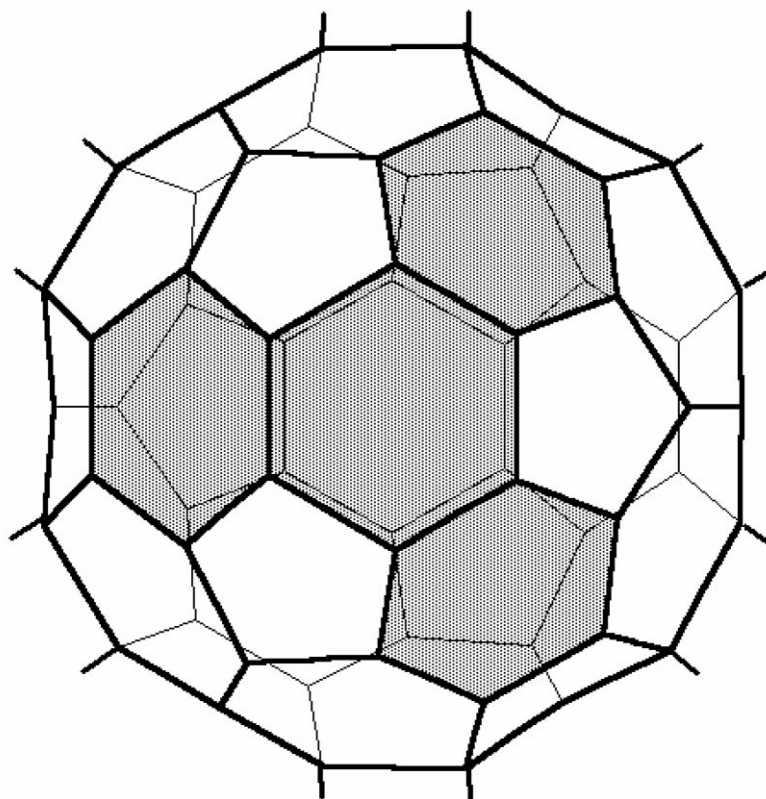


Fig. 11. Schematic representation of the crystal orbital accompanied by the small-dispersed band from the electronic structure of the hexagonal polymer. The electronic density from this orbital is localized on the dashed hexagons.

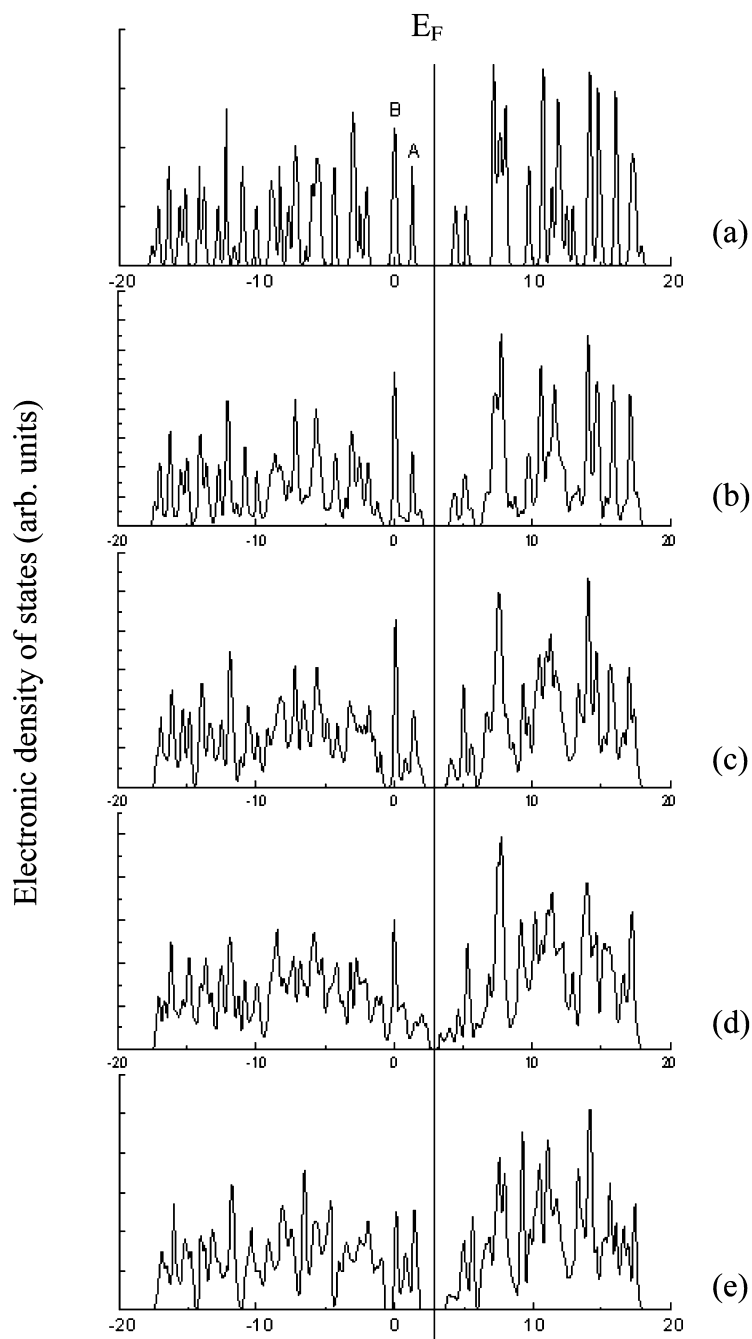


Fig. 12. Calculated electronic density of states for icosahedral  $C_{60}$  molecule (a), linear  $C_{60}$  chain (b), 2D tetrahedral (c) and hexagonal (d) polymers, 3D  $C_{60}$  polymer (e).

originates from the HOMO of  $h_u$  symmetry and the feature B corresponds to two lower energy orbitals having  $h_g$  and  $g_g$  symmetries. From the icosahedral molecule to the hexagonal polymer the intensity of these features is gradually decreased. The feature A is considerably broadening,

while the width and intensity of the feature B are less varying. The 2D hexagonal polymer is characterized by the most noticeable changes of these features, that is due to the largest change of  $p$ -system of the icosahedral  $C_{60}$  when a hexagonal layer is formed. This considerable change is also the cause

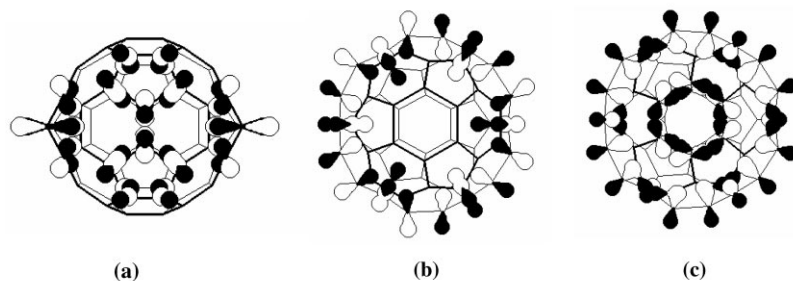


Fig. 13. The examples of the crystal orbitals providing  $\sigma$ -bonding between neighboring  $C_{60}$  cages in the linear polymer (a) and the hexagonal layer (b,c).

Table 2

Energetic characteristics of icosahedral  $C_{60}$  molecule and the polymerized fullerite forms: the calculated HO–LU band gap ( $E_g$ ), total ( $E_{tot}$ ), electronic ( $E_{bs}$ ) and repulsive ( $E_{rep}$ ) energy

Structure	$E_g$ (eV)	$E_{rep}$ (eV/atom)	$E_{bs}$ (eV/atom)	$E_{tot}$ (eV/atom)
Icosahedral $C_{60}$	3.101	12.175	–28.265	–16.090
Linear chain	2.180	11.607	–27.612	–16.005
Tetragonal layer	1.852	11.171	–27.093	–15.922
Hexagonal layer	0.577	11.468	–27.119	–15.651
Cubic	2.235	10.482	–26.707	–15.865

of the smallest energy gap between the bands, whose density forms the features A and B, and the deeper occupied bands. The features A and B in the electronic DOS are associated with the bands from the blocks A and B, therefore, the decreasing their intensities reflects the reduction of the number of localized orbitals. The localization of electron density from the higher occupied COs on the individual  $C_{60}$  cage of the cubic polymer gives the intense feature near the Fermi level.

The population analyses has shown that the intermolecular bonds in the  $C_{60}$  polymers are almost pure  $\sigma$ -bonding. The orbitals providing the  $\sigma$ -bonding between carbon cages are positioned in the depth of valence band about of 8–9 eV below the Fermi level. The examples of such type COs in the 1D and hexagonal polymers are given in Fig. 13. Two orbitals, which are differed by a sign of the AOs overlapping in the four-membered ring, are divided in the electronic structure of the linear  $C_{60}$  chain. As evident from Fig. 13(a), radially directed AOs form the  $\rho$ -type orbital. In the electronic structure of the tetragonal polymer there are COs, providing the  $\sigma$ -bonding between molecules or simultaneously along both the crystallographic directions ( $x,y$ ) or along a particular one. The intermolecular  $\sigma$ -bonding COs of the hexagonal polymer can be as pure  $\rho$ -type orbitals (Fig. 13(b)) thus a combination of radial and tangential AOs (Fig. 13(c)). Through the former orbital, the AOs of the atoms composing the four-membered rings have the positive overlapping between molecules and negative overlapping on the other directions. The latter CO being completely bonding is energy deeper orbital.

### 3.6. Energy of the polymeric structures

The calculated HO–LU band gap and energies  $E_{tot}$ ,  $E_{bs}$ , and  $E_{rep}$  for the polymerized fullerite forms are compared with those of free  $C_{60}$  molecule in Table 2. The total energy of each of the considered polymeric structure is higher than that of the fullerene molecule. By increasing the neighbors in a polymer its total energy increases, except that for the three-dimensionally polymerized  $C_{60}$ . Analysis of the  $E_{bs}$ , and  $E_{rep}$  values shows that the less stability of the hexagonal polymer compared to the cubic one is caused by the stronger short-range repulsion in the former structure. Actually, the more closely packing of the  $C_{60}$  cages in the hexagonal layer than in any plane of the cubic structure leads to the additional interactions, in particular, the intermolecular  $\rho$ -electron overlapping. The change of the total energy with the polymerization correlates with the change of the HO–LU band gap: than the band gap is smaller that the polymer is less stable.

## 4. Conclusion

The tight-binding method was parameterized to correct reproducing the 2p-electron density distribution in the valence band of the fullerite  $C_{60}$  and  $C_{70}$ . The determined parameters can be used later for the electronic structure investigation of various cage carbon compounds and the calculation of X-ray emission and photoemission spectra for them. However, as evident from the energy gap

overestimation in the  $C_{60}$  polymers, the re-parameterization impaired description of the electron interactions in the conductance band and conducting properties of a compound may be predicted from the comparative calculations only. Using new parametric scheme, a systemic study of electronic band structure of four polymerized phases of  $C_{60}$ , which are known today, was carried out. For the tetragonal and rhombohedral phases only one layer was calculated assuming the insignificant influence of van der Waals interactions between layers on the electronic energy bands and crystal orbitals.

Polymerization of fullerene  $C_{60}$  results in the narrowing of HOMO–LUMO gap that is caused by the splitting of the degenerated MOs of the icosahedral  $C_{60}$  due to its distortion and the formation of intermolecular bonds. All considered polymers were found to be semiconductive with the smallest band gap for the 2D hexagonal polymer and the largest one for the cubic polymer. A change of the band gap with the number of neighbors and the type of their connection in the polymer correlates with the calculated total energy values. The polymerized fullerite forms were found to be less stable than free  $C_{60}$  molecules. Among the polymers, the linear  $C_{60}$  chain is characterized by the greatest energy stability.

Near the Fermi level, the  $\rho$ -type crystal orbitals, whose electronic density is localized on individual  $C_{60}$  cages, were revealed for all calculated polymers. The number of such orbitals decreases when the number of neighbors and the extent of  $C_{60}$  fragment distortion increases. The  $\sigma$ -bonding between  $C_{60}$  molecules was found to provide by the crystal orbitals located about 8–9 eV below the Fermi level. Furthermore, due to the small-size cavities in the hexagonal layer, intermolecular interactions are also provided by the highest  $\rho$ -orbitals. The analyses of the frontier orbitals in the polymeric chain and the tetragonal structure showed the further attachment of fullerene molecules should result in the formation of tetragonal and cubic polymers, respectively.

### Acknowledgements

This work was financially supported by the Russian scientific and technical program “Fullerenes and Atomic

Clusters” (Projects no. 5-1-98), and Federal Directed Program “Integration”, grant K0042.

### References

- [1] Y. Iwasa, T. Arima, R.M. Fleming, T. Siegrist, O. Zhou, R.C. Haddon, L.J. Rothberg, K.B. Lyons, J.r. Carter, L. H, A.F. Hebard, R. Tycko, G. Dabbagh, J.J. Krajewski, G.A. Thomas, T. Yagi, *Science* 264 (1994) 1570.
- [2] M. Nunez-Reguerio, L. Marques, J.-L. Hodeau, O. Bethoux, M. Perroux, *Phys. Rev. Lett.* 74 (1995) 278.
- [3] G. Oszlanyi, L. Forro, *Solid State Commun.* 93 (1995) 265.
- [4] L. Marques, J.-L. Hodeau, M. Nunez-Regueiro, M. Perroux, *Phys. Rev. B* 54 (1996) R12633.
- [5] V.D. Blank, S.G. Buga, N.R. Serebryanaya, V.N. Densiov, G.A. Dubitsky, A.N. Ivlev, B.N. Mavrin, M.Yu. Popov, *Phys. Lett. A* 205 (1998) 208.
- [6] P.-A. Persson, U. Edlund, P. Jacobsson, D. Johnels, A. Soldatov, B. Sundqvist, *Chem. Phys. Lett.* 258 (1996) 540.
- [7] C. Gonze, F. Rachdi, L. Hajji, M. Nunez-Rugueiro, L. Marques, J.-L. Hodeau, M. Mehning, *Phys. Rev. B* 54 (1996) R3676.
- [8] A.M. Rao, P.C. Eklund, J.-L. Hodeau, L. Marques, M. Nunez-Regueiro, *Phys. Rev. B* 55 (1996) 4766.
- [9] M. Sundqvist, *Physica B* 265 (1999) 208.
- [10] A. Ito, T. Morikawa, T. Takahashi, *Chem. Phys. Lett.* 211 (1993) 333.
- [11] K. Tanaka, Yu. Matsuura, Y. Oshima, T. Yamabe, Y. Asai, M. Tokumoto, *Solid State Commun.* 93 (1995) 163.
- [12] C.H. Xu, G.E. Scuseria, *Phys. Rev. Lett.* 74 (1995) 274.
- [13] S. Okada, S. Saito, *Phys. Rev. B* 55 (1977) 4039.
- [14] S. Okada, S. Saito, *Phys. Rev. B* 59 (1999) 1930.
- [15] S. Okada, S. Saito, A. Oshiyama, *Phys. Rev. Lett.* 83 (1999) 1986.
- [16] D. Tomanek, S.G. Louie, *Phys. Rev. B* 37 (1988) 8327.
- [17] A.V. Okotrub, L.G. Bulusheva, *Fullerene Sci. Technol.* 6 (1998) 405.
- [18] S. Saito, A. Oshiyama, *Phys. Rev. Lett.* 66 (1991) 2637.
- [19] L. Goodwin, A.J. Skinner, D.G. Pettifor, *Europhys. Lett.* 9 (1989) 701.
- [20] C.H. Xu, C.Z. Wang, C.T. Chan, K.M. Ho, *J. Phys.: Condens. Matter* 4 (1992) 6047.
- [21] A.V. Okotrub, L.G. Bulusheva, Yu.V. Shevstov, L.N. Mazalov, O.A. Gudaev, V.K. Malinovskii, *Phys. Low-Dim. Struct.* 5/6 (1997) 103.